Design and optimization strategy of HAWT using a local pitch angle adaptation

Issam Meghlaoui[1,2], Toufik Madani Layadi[1,3]

[1]Laboratory of Materials and Electronic Systems, Department of Electromechanical, Faculty of Sciences and Technology,
University Mohamed El Bachir El Ibrahimi of Bordj Bou Arreridj, El Anasser, Algeria
[2]Arts et Métiers-ParisTech, LIFSE, Paris, France
[3]University of Poitiers, ISAE-ENSMA Poitiers, LIAS, France

Article Info

ABSTRACT

In this paper, a smart design of a horizontal wind turbine (HAWT) has been developed. The developed design allows improving kinetic energy recuperation with high efficiency. The considered design of the wind turbine is characterized by a specific mechanical structure of blades. Each blade contains separated elements with an adaptable local pitch angle. To develop the smart wind turbine, a new algorithm for controlling the blade elements has been implemented. It allows estimating the distribution of the twist angle of each blade element. The achieved twist angle corresponds to the extracted optimal power provides by the wind turbine. The obtained results show a significant improvement relative to the wind turbine power coefficient under operating conditions. In fact, for some rotating velocity, the rate of this coefficient is increased by 21%. Moreover, notable kinetic energy recuperation is observed. Furthermore, smart orientation of elements proved optimal energy recuperation for a large scale of tip speed ratio and wind speed. In addition, the proposed structure of the wind turbine is more beneficial to minimize the axial thrust. Furthermore, the axial thrust of the wind turbine has been decreased by 21% for some operating velocity and specific conditions. As perspectives for the future works many ideas are suggested.

Corresponding Author:

Toufik Madani Layadi
Laboratory Materials and Electronic Systems, Department of Electromechanical
Faculty of Sciences and Technology, University Mohamed El Bachir El Ibrahimi of Bordj Bou Arreridj
34030 El-Anasser, Bordj Bou Arreridj, Algeria
Email: toufikmadani.layadi@univ-bba.dz

1. INTRODUCTION

Generally, wind turbines have a specific form of blades [1]. Also, wind turbines are designed to operate according to well-defined meteorological data of sites [2]. These meteorological data can be ambient temperature with climate variations of the weather (ice and rain), and wind speed. In fact, the permanent variations of wind speed and load profile of the turbine can change the optimal operating point of the whole system. Operating out of optimal point can cause losses of energy recuperation [3], [4]. Avoiding this kind of phenomena, many solutions can be proposed [5], [6], such as maximum power point tracking (MPPT) technique [7]-[11]. This technique is used to maximize the recuperated power of wind turbines. Energy recuperation is based on implementation of control algorithms. However, this optimization technique is considered limited by the mechanical architecture of the wind turbine. Also, other optimization techniques of control have been proposed to maximize energy recuperation, which are active [12]-[14] and passive [5], [15]

control techniques. The active one is subdivided into two different techniques. The first technique is called individual pitch control [16], [17], which focuses on an independent variation for each blade of the wind turbine. Each blade can be pitched by a specific angle. The proposed technique allows minimizing significantly the stress phenomenon of blades. However, implementation of this technique on real situation is not commercially suggested. The second one is nominated the global pitch control technique [18] and represents the most known conventional optimization technique. In this technique all blades receive the same control angle, which increases the stability of the wind turbine. Until know the last technique is mostly used to control most wind turbines. In fact, it allows optimizing the aerodynamic of kinetic energy recuperated by the wind turbine. The passive control technique focuses on mechanical adaptation of wind turbine blades. Many researchers have interested to develop this control technique for horizontal wind turbines (HAWT) to incline the blades of wind turbines. This technique is based on using forces and torques that can be generated naturally by the wind. Also, they affect the rotor shape of wind turbine [19]-[21]. Some elements like spoilers, deflectors or flexible leading edges are generally used in passive control technique [22]-[24]. These elements are designed to modify passively the aerodynamic force distribution along the blades. This modification can influence the angle of attack and decrease the load fluctuations. Moreover, it allows not only to stabilize the wind turbine against the wind variation, but also to optimize the wind energy efficiency, and minimize the losses of production that caused by meteorological condition variations. Implementation of the passive technique requires advanced materials of production with complex manufacturing. Recently, some research works have investigated to optimize the blade design of HAWT [25]-[28]. This optimization is implemented for a specific rotational and a well-defined wind speed.

According to the wind turbine architecture, each blade element participates to generate its propre torque dQ. This torque is generated through resulting forces acting on the blade elements. Forces that act on the airfoil sections of the blades depend on several parameters such as chord length: airfoil section, wind speed, rotational velocity and inflow angle φ. This angle plays important role to achieve significant energy recuperation [29]. The angle is calculated by using wind speed and rotational velocity of the wind turbine. Under operating conditions this angle can be changed and causes a clear diminution in power recuperation. Also, it causes a significant increase in the axial thrust on wind turbine structure.

The goal of the present research work is to develop a new design for HAWT. The proposed wind turbine design can adapt smoothly the pitch angle along the blade. The new configuration of the wind turbine is based on subdividing the blade into many elements. Each element is pitched individually to reach the optimal configuration; and improve the wind turbine efficiency. Controlling of the blade elements is realized using a powerful control algorithm. This algorithm can find the optimal local pitch angle for each element and adapt it according to external data variations (wind speed and rotational speed). Development, implementation and simulation of the proposed wind turbine is performed in MATLAB-Simulink environment. Simulation results demonstrate clearly the smart configuration improvements comparing to the conventional one.

This paper is organized as follow: first, materials and methods are presented in section two. In this section, the main idea of the proposed model and mathematical models are shown. Different case studies with important simulation results are mentioned in section three. Furthermore, significant clarifications about the obtained results are added. Finally, conclusion and perspectives are presented.

2. METERIALS AND METHOD

In this section, many sub-sections are presented to develop the main idea of the contribution.

2.1. Description and design of the proposed blade

To maximize the wind turbine rotor performances, it is crucial to optimize the local pitch angle of the blade elements. Each blade comprises several elements as shown in Figure 1. These elements are mounted together to form a malleable and smooth geometry. However, each element can be twisted individually to improve the energy recuperation, and to decrease the axial thrust acting on wind turbine.

2.2. Case study of wind turbine

The selected wind turbine is a horizontal bi-blade turbine. Figure 2 illustrates the chord length distribution along the blade radius. It is observed that the chord section along the radius is increased around the root of the blade and decreased around the tip region. Table 1 shows the wind turbine model parameters such as density, kinematic viscosity of air, tip speed ratio and wind speed range. To extend the wind turbine simulation, a large interval of tip speed ratio and wind speed values are considered.

Generally, small wind turbines use one aerodynamic profile along the blade. However, according to some research works, many profiles of different airfoil sections can be used [25]. Increasing airfoil section at

the root region allows the wind turbine rotor resisting against high constraints and axial thrust. However, thin airfoil sections are suggested for the tip region. In the present study, elements along the blade are considered have the same airfoil section NACA 4412. These profiles are the most used to design the wind turbine blades. They have a significant lift-to-drag coefficient ratio. Table 2 depicts the airfoil NACA 4412 and its parameters.
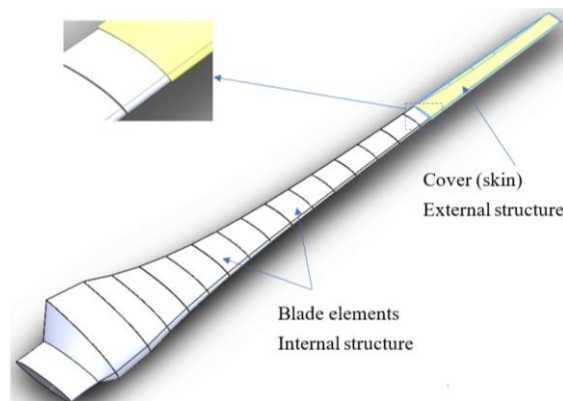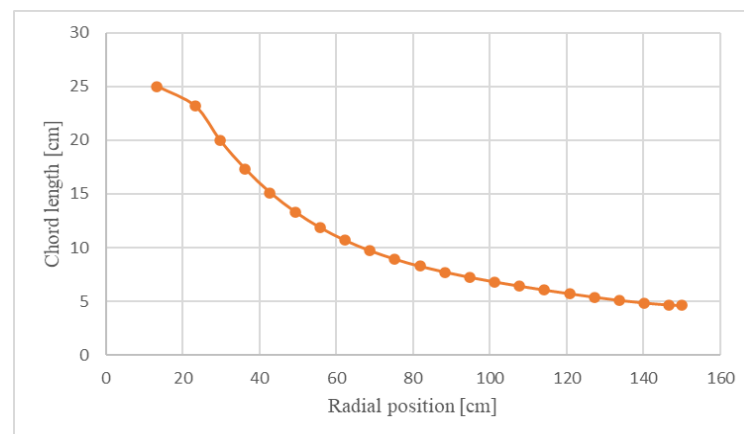

Figure 1. The proposed structure of the blade

Figure 2. Chord length vs. radial position for the studied wind turbine

Table 1. Wind turbine model parameters

Atmospheric parameters	Value/unit	Blade parameters	Value/unit
Density of air ρ	1.25 (Kg/m^3)	Number of blades N_b	2 (-)
Viscosity of air $\mathcal{V}$	1.87 10^{-5} (m^2/s)	Tip speed ratio TSR	6-14 (-)
Atmospheric pressure P_{atm}	990 (hPa)	Airfoil NACA	4412
Wind speed U_0	6-14 (m/s)	R_{tip}	1.5 (m)

Table 2. Aerodynamic parameters of the airfoil

Parameter/airfoil	NACA 4412
Airfoil thickness, th (%)	12
Lift coefficient, C_l (-)	1.2
Drag coefficient, C_d (-)	0.012
Angle of attack, α (°)	6.5

2.3. Local twist angle extraction

To extract the optimal value of the local pitch angle, the blade element momentum method has been adopted for each blade element. Implementation of the proposed method is based on (1) and (2).

$$\lambda_r = (4a - 1)((1 - a)(1 - 3a')^{-1})^{1/2} \tag{1}$$

$$a' = (1 - 3a)(4a - 1)^{-1} \tag{2}$$

Where the local speed ratio λr is expressed in function of the axial and tangential induction factors a and a' respectively. The optimal twist angle β is expressed as:

$$\beta = \varphi - \alpha \tag{3}$$

Where α is the angle of attack. The flow angle φ is calculated in function of wind speed U_0 and the angular rotor speed Ωr as:

$$\varphi = tan^{-1}[(1 - a)U_0((1 + a')\Omega r)^{-1}] \tag{4}$$

The previous equations are used to obtain the twist angle β. This angle is ideal for a equals $1/3$, and for a' equals zero. Adaptation of this angle will be realized using iterative calculation. The calculation algorithm uses this angle as an input. The main iterations of the algorithm are detailed in sub-section 2.7.

2.4. Implementation of the blade element method

Figure 3 shows the relationship between aerodynamic forces, velocity and angles [30], [31]. Using vectorial presentation given in Figure 3 several equations are obtained. In (5) and (6) demonstrate respectively normal force coefficient C_n, and tangential force coefficient C_r as:

$$C_n = C_l \cos \varphi + C_d \sin \varphi \tag{5}$$

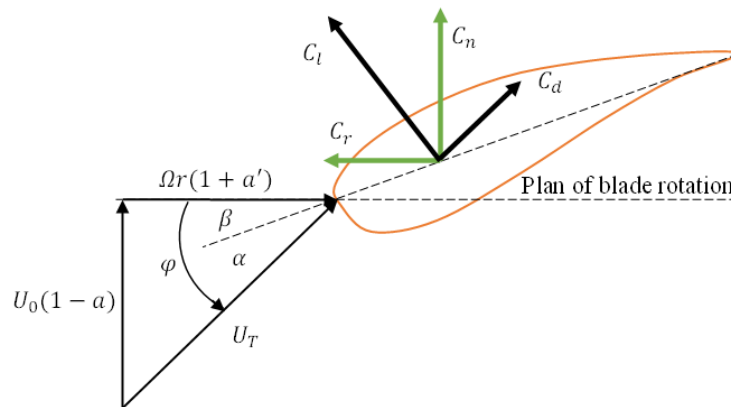$$C_r = C_l \sin \varphi - C_d \cos \varphi \tag{6}$$

Figure 3. Vectorial presentation of aerodynamic forces, velocities and angles

The thrust coefficient C_t and torque coefficient C_Q are given as:

$$C_t = U_T^2 C_n L_c N_B (2\pi r U_0^2)^{-1} = \sigma C_n U_T^2 (U_0^2)^{-1} \tag{7}$$

$$C_Q = U_T^2 C_r L_c N_B (2\pi r U_0^2)^{-1} = \sigma C_r U_T^2 (U_0^2)^{-1} = C_t C_r (C_n)^{-1} \tag{8}$$

where, U_T represents the relative wind velocity and σ is the solidity factor of the wind turbine.

$$\sigma = L_c N_B (2\pi r)^{-1} \tag{9}$$

The tangential induction factor a' is expressed as:

$$a' = C_Q (4(1 - a)\lambda_r)^{-1} \tag{10}$$

where,

$$\lambda_r = \Omega r (U_0)^{-1} \tag{11}$$

Some improvements are added to correct the infinite number of blade assumptions [32], [33]. In the present study the tip loss factor is implemented as:

$$F = \frac{2}{\pi} \cos^{-1} \left[e^{-\frac{N_B}{2} \left(\frac{Rtip-r}{r \sin \varphi} \right)} \right] \tag{12}$$

2.5. Local twist angle adaptation for different radial positions

To maximize the recuperated power of wind turbines, the axial induction factor a must be close to its ideal value 1/3 for the different blade elements. So, the twist angle of elements should be adapted to optimize the axial induction factor value. Figure 4 demonstrates the twisting of the blade. Also, many profiles are presented, and each profile is characterized by its chord length and a specific twist angle. It means, the twist angle of the blade presents the torsion of the blade. Due to the high $U_0/\Omega r$ ratio, it is known that the airfoil section at the root region is twisted into the wind [34]. However, the blade tip is generally perpendicular relative to the wind. The rotational speed and wind speed velocity can define the inflow angle of the air stream at a specified radius. In fact, the required local twist angle must be updated in real time with U_0 and Ω.
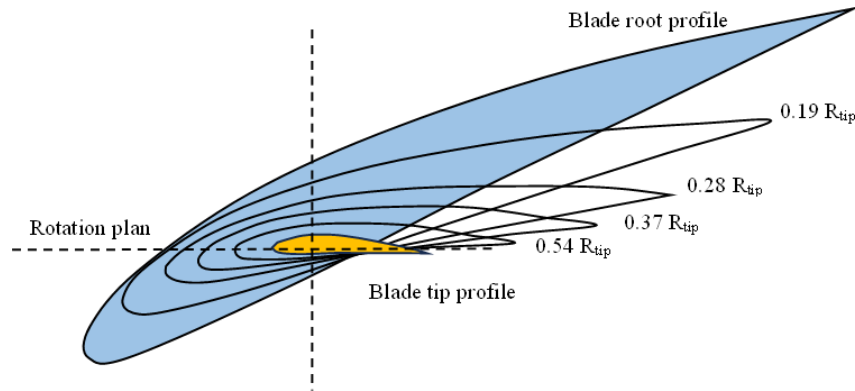

Figure 4. Local twist of the wind turbine blade for different radial positions

2.6. Power and force evaluation

To evaluate the local rotor thrust force dT and torque dQ, mathematical expressions have been used as:

$$dT = \frac{1}{2} N_B L_c C_n \rho U_0^2 (1-a)^2 (\sin \varphi)^{-2} dr \tag{13}$$

$$dQ = \frac{1}{2} N_B L_c C_r \rho U_0 (1-a) r\Omega (1+a') (\sin \varphi \cos \varphi)^{-1} dr \tag{14}$$

The global calculation of the total thrust force T, torque Q, and rotor shaft power P_{rotor} are expressed by the following expressions.

$$T = \int_{R_{hub}}^{R_{tip}} dT dr = \sum_{i=1}^{N_{el}} dT_i \Delta r \tag{15}$$

$$Q = \int_{R_{hub}}^{R_{tip}} dQ r dr = \sum_{i=1}^{N_{el}} r_i dQ_i \Delta r \tag{16}$$

$$P_{rotor} = Q\Omega \tag{17}$$

Finally, the power coefficient C_p of the wind turbine and the thrust force coefficient C_t are shown as:

$$C_p = Q\Omega \left(\frac{1}{2}\rho U_0^3 A\right)^{-1} \tag{18}$$

$$C_t = T \left(\frac{1}{2}\rho U_0^2 A\right)^{-1} \tag{19}$$

Where, A represents the area of the rotor.

2.7. Operating algorithm description

Algorithm calculation needs necessary inputs which are tip speed ratio (TSR), number of blades, chord length, radius and speed of rotor, and atmospheric parameters such as wind speed, air density and viscosity. By using the blade element method and iterative calculation, the induction factors (*a* and *a'*) are evaluated. When these factors reach the optimal value, the algorithm stops its calculation. By the end of evaluation, and for each element of blade, the algorithm can extract the force coefficients and the flow angle. Based on the obtained values, the algorithm starts a new stage of calculation. In this stage, the local twist angle is evaluated iteratively by the algorithm to obtain the optimal value reaching the maximum power coefficient.

In conclusion, the local twist angles are updated for each blade elements. Hence, the optimal twist angles provide a new shape for the blade. Furthermore, the targeted parameters of the blade, power coefficient, and axial thrust coefficient are extracted.

3. RESULTS AND DISCUSSIONS

In this section several simulation tests have been realized. To clarify the importance of the proposed algorithm, many suggestions are considered.

3.1. Analysis relative to axial induction factor

Generally, the axial induction factors *a* represents a reliable indicator to evaluate the recuperated power from the wind turbine. In fact, in terms of power, each element has a proper local axial induction factor. Following the wind turbine theory, the local axial induction factor of each element should be equal to 1/3 to reach the optimal power. The proposed algorithm considers the twist angle optimization. To obtain the optimal power from the wind turbine, it is crucial to optimize the local induction factor of each element. Figure 5 shows the axial induction factor values *a* along the normalized blade radius for different TSR. Figures 5(a) to 5(d) demonstrate the axial induction factor relative to normalized blade radius for TSR equals 10, 14, 13 and 12 respectively. For each TSR values, three curves are given. The green curve represents the ideal demonstrated value of axial induction factor. This curve is considered as the reference value. In cases (a), (b), (c), and (d), wind speed is supposed equals 10 m/s.

Comparing between curves, red color reflects the conventional configuration of the wind turbine. In fact, when TSR is augmented, the local axial induction factor is far away relative to the theorical value along the wind turbine radius. In fact, for TSR equals 14, the difference between the simulation curves and the theorical assumption (green curve) is increased by 50% along the blade radius.

The blue curve shows the smart configuration of the blade. Its variation follows with precision the ideal curve for a large zone of TSR. The present results demonstrate significant improvements. The achieved results provide an optimal axial induction factor along the blade radius for a wide range of TSR. In addition, the finding results show that most blade sections operate around airfoil optimum angle of attack. However, in the previous study presented in [25], only one value or a narrow range of TSR is considered. For TSR equals to 10, 12, and 13, a clear deviation between curves at the tip blade is observed. This deviation due to the influence of the tip loss factor implemented in the BEM method. The Tip loss factor importance is discussed in [32] and [33].

In the proposed solution, the local twist angle for each element of the blade should be adapted in real time in function to the angular speed, and the wind speed. Figure 6 depicts the local twist angle variation along the normalized blade radius for different TSRs. The presented curves illustrate the local twist angle values that are obtained from the simulation experiences. Also, a graphical comparison between the local twist angles of conventional and the smart structures at wind speed U0 = 10 m/s is proved. It is observed that there is a clear gap between both structures. A value of -7.46° is extracted around the root of the blade, and a value of + 1.49° is achieved from the tip of the blade for TSR equals 14. In addition, for TSR equals 13, a value of -5.6° is estimated around the root, and a value of +2.52° is calculated around the tip.

For each TSR, it is proved that each blade section with its proper twist angle is different relative to the adjacent section. The obtained results demonstrate that the proposed technique is more significant than conventional ones, such us global pitch control technique where, all sections of the blade have the same

twisted angle [16], in fact the proposed algorithm can control separately the orientation angles of the blade sections. Hence, all blade elements working around an optimal angle of attack over a large range of TSR.
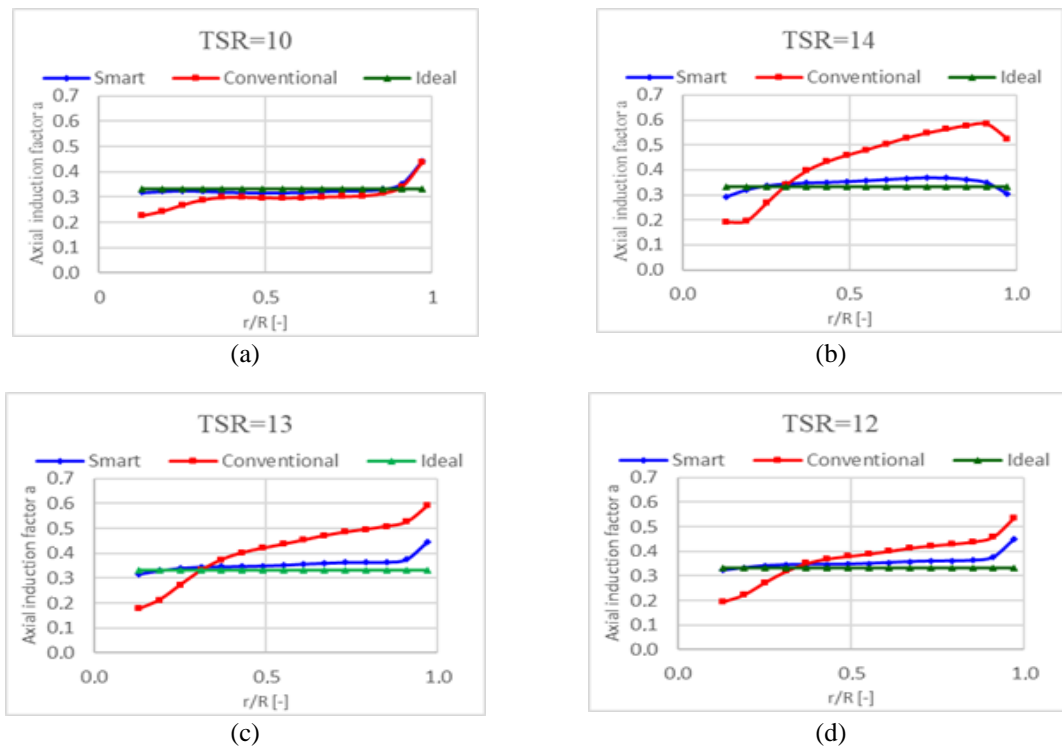

Figure 5. Local axial induction factors along the normalized blade radius for conventional and smart geometries at a wind speed of 10 m/s for different: (a) TSR=10, (b) TSR=14, (c) TSR=13, and (d) TSR=12
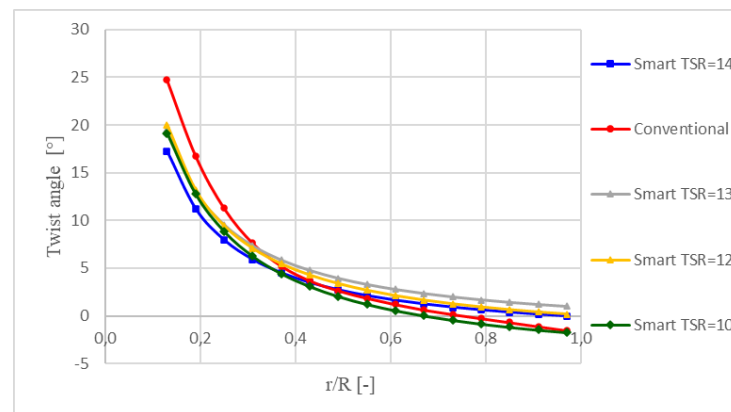

Figure 6. Local twist angle along the normalized blade radius at a wind speed of 10 m/s for different TSR

Figure 7 shows the airfoil section along the normalized blade radius for different TSR at a wind speed of 10 m/s. The blue profiles represent root blade elements. However, the orange one illustrates the tip blade elements. It is observed that there is a significant changing in the geometric form of the wind turbine blade for different rotational speeds. The local twist angle changing is increased progressively from the tip to the root of the blade for low TSR values. For instance, when TSR is low, the local twist angles between elements are increased which causes more torsion of the blade. To clarify the difference between the conventional and smart design of the blade, superposition of two geometries is presented for TSR=10.

A significant deviation between the twist angle values around the root region of the blade is observed. These results are more significant and demonstrate practically the way how the blade shape is

changing progressively for a large operating zone where, TSR=6 to TSR=14. In practical case, implementation of the proposed structure needs mechanical articulations, and actuators that ensure an individual twist of each section of the blade. In contrast, the conventional design of blade has a solid geometry. In this case, one twist angle is given along blade [25].
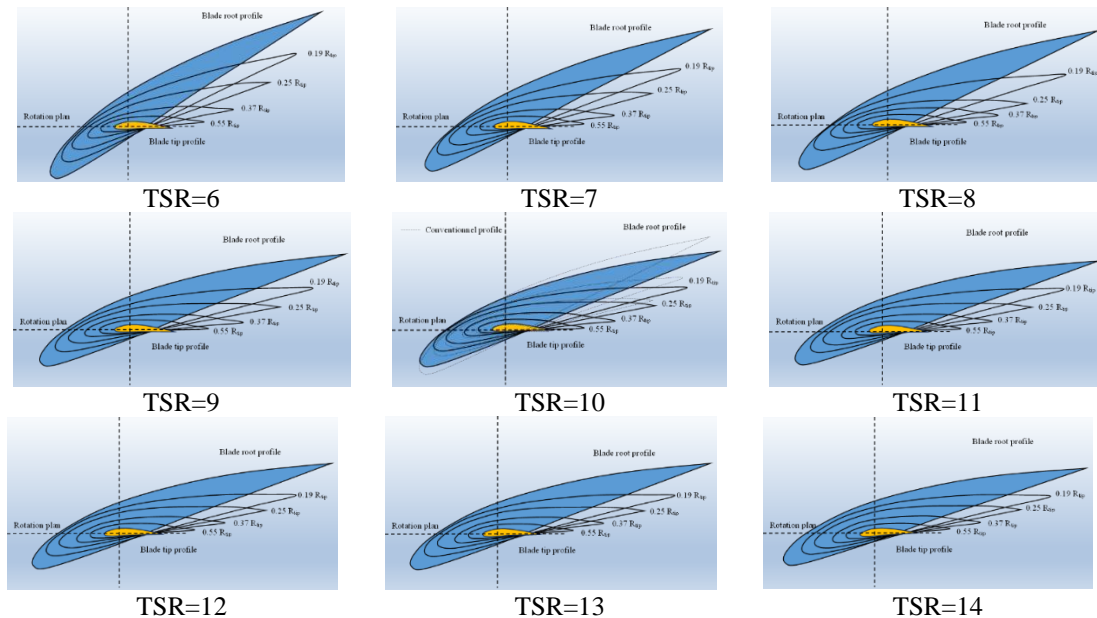

Figure 7. Profile view of the blade for different tip speed ratio and normalized radius at a wind speed of 10 m/s

3.2. Analysis and Performance study

Figure 8 demonstrates power and axial thrust coefficient curves in function to TSR. C_p and C_t curves are obtained from experiment simulations for smart and conventional configurations, where the wind speed U_0 is equal to10 m/s. Extraction of power coefficients is based on implementation of blade element momentum method (BEM) in MATLAB/Simulink environment for a large scale of TSR. According to C_p curves, the smart configuration provides a wide space of power recuperation with high performances.

Figure 8(a) proved the best performance of C_p for TSR equals 9 in smart configuration. In fact, the C_p value reached 46.40 %. When TSR is upper than 11, the smart configuration illustrates important C_p values than the conventional one. In fact, around TSR=14, the deviation of C_p value corresponds to 14.65% relative to the smart design. The obtained results demonstrate that the flexible blade geometry is more significant than the rigid one in terms of energy recuperation and performances. In fact, the study presented in [35] and [36] proved that flexible structure outperforms rigid one.

Figure 8(b) presents the Ct coefficient comparison between the different configurations. It is observed that in conventional design, the axial thrust coefficient is exceeded the unity value for a high TSR. However, in the smart configuration, the axial thrust coefficient is considered limited at 0.9. For TSR equals 14, the smart configuration can minimize the axial thrust force by 18,62 %. Furthermore, smart adaptation of local pitch angles allows minimizing considerably the axial force impact on the wind turbine. This finding supports the idea of the research work presented in [29]. Moreover, the thrust is decreased when the pitch angle increased. In the practical aspect, the proposed technique allows protecting the wind turbine against the stress and increasing durability and blade lifetime.

Generally, optimal design of wind turbine blades is performed according to a specific TSR and wind speed. However, wind speed variations can cause the wind turbine to work out of optimal zone. To generalize the study of performances, it is essential to extend the study by evaluating the relationship between thrust coefficient, power coefficient and local twist angle for different TSRs and wind speeds on a large scale. Figure 9 depicts variations of power coefficient in function of TSR and wind speed. To analyze the power coefficient, two curves are superposed as given in Figure 9(a). This superposition allows to differentiate between smart and conventional geometries. In addition, it is observed that the smart curve represents the upper envelop for the conventional one. Also, the smart geometry illustrates a large working zone with high performances for different values of TSRs and wind speeds. In this case study, the TSR is comprised between

6 and 14, where wind speed U_0 is comprised between 6 m/s and 14 m/s. orange curve defines the power coefficient with high values (42%). The finding results relative to TSR, and wind speed parameter represent significant improvements. These improvements are evaluated by high values of C_p where, the wind turbine can exploit a large zone of working. To clarify the variation of power coefficient gap between the proposed geometry and the conventional one, a new graphical curve is shown in Figure 9(b). For high TSR values (TSR>12), a rate of 15% of power coefficient can be gained for different wind speeds. From Figure 9(b), it is noted that the maximum power recuperation reached 21% for TSR equals 14 and a wind speed value equals 14 m/s. Following the finding results significant improvements have been achieved under high TSR values. However, the gained power does not exceed 5% for low TSR values, and for different wind speeds. In fact, for low TSR values, high angles of attack favorize the aerodynamic stall for the majority of blade sections.
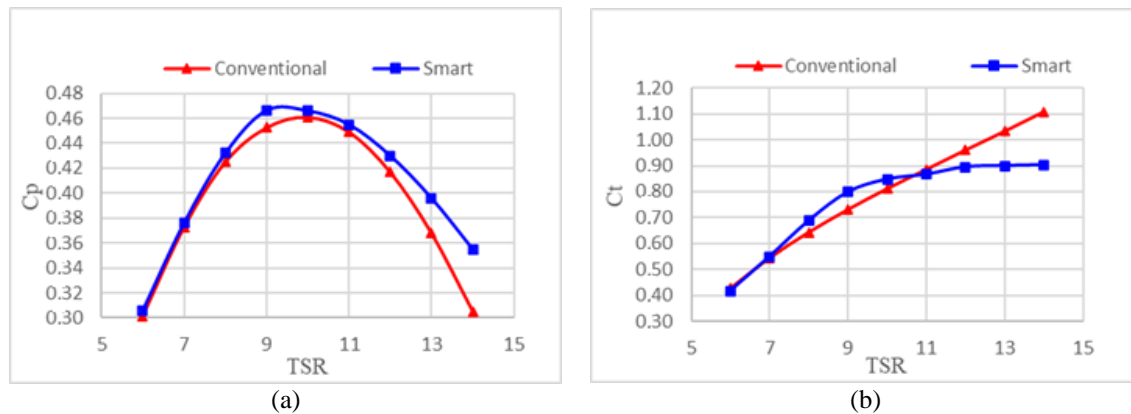

Figure 8. Wind turbine coefficients vs. TSR at a wind speed of 10 m/s using BEM for different design
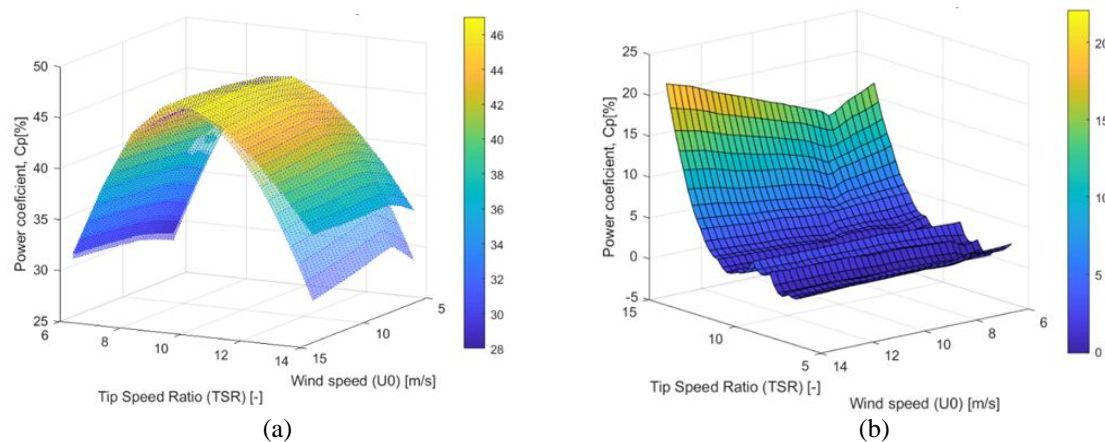(a) power coefficient vs. TSR and (b) thrust coefficient vs. TSR

Figure 9. Power coefficient evaluation for wind turbine geometries (a) power coefficients vs. TSR and wind speed and (b) difference between power coefficients vs. TSR and wind speed

Figure 10 demonstrates the axial thrust coefficient in function of TSR for different wind speeds. Superposition of axial thrust curves extracted from experiment simulations is illustrated in Figure 10(a). The linear curve given represents the conventional geometry, and the lower one shows the smart configuration. When the TSR is upper than 10, the smart geometry represents weak axial thrust coefficients C_t<0.9 for all wind speed values comparing to the conventional configuration where, C_t exceeds the unity. The results proved significant values comparing to the advanced pitch angle control using genetic algorithm technique presented in [36]. The obtained findings show a strong relationship between the twist angle and the axial thrust. In fact, this relationship is confirmed in the research work given in [29]. Hence, its observed that the thrust is decreasing with increasing of pitch angle due to reduction in frontal area. Figure 10(b) depicts important attenuation in the axial thrust, and its value is estimated by 21% for TSR=14 and U0=14m/s. In

addition, for TSR>12, the axial thrust is reduced by 10% for all wind speeds. For TSR<8, local angles of attack for the blade sections can reach Stall limit [25]. In this case, the optimization algorithm become unable to find more improvements in local twist angles. Under this situation, the attenuation is limited to 5% for different wind speeds.

Figure 11 shows clearly the local twist angle distribution for different TSR along the normalized radius at a wind speed of 10 m/s. Figure 11(a) depicts the difference between local twist angle for smart and conventional geometries. Figure 11(b) shows the difference between local twist angles for the different geometries in terms of TSR. According to the transparent curve given in Figure 11(a), it is observed that the root elements (*r/R*<0.4) have the highest twist angle range comparing to other elements. For instance, local pitch angle that varied within 17.83° at TSR=11 to 30.46° at TSR=6 shows the case. Also, for TSR equals 11, the twist angle deviation between the conventional structure and the smart one can reach the value of 6.88° as given in Figure 11(b). Then, the obtained results provide an adaptable design of the root region. So, the optimized design of the root region of the blade is considered crucial to facilitate the starting of the modern wind turbine [37]. Following Figure 11(a), the local twist angle is varied within 2.88° at TSR=9 to 0.84° at TSR=14 around the tip of blade. Also, the twist angle deviation extracted between the conventional structure and the smart one is equal to -2.73° at TSR=14 and equal to 1.35° at TSR=9 as presented in Figure 11(b). Hence, these findings are in line with Clifton-Smith conclusion that demonstrates the importance of the tip region [38]. In fact, the tip of blade is considered as the efficient region in terms of energy recuperation, where the most part of aerodynamic torque is provided by the elements of the blade tip.
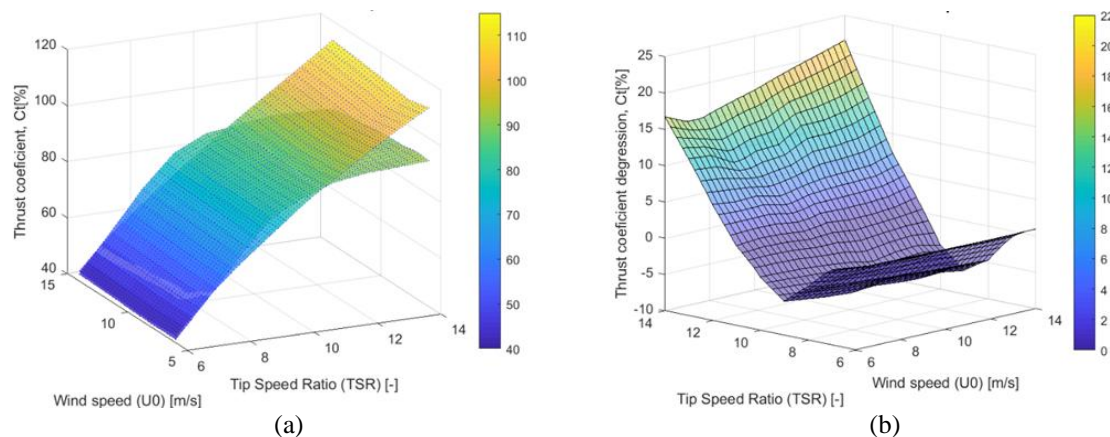

Figure 10. Axial thrust coefficients evaluation for both geometries (a) thrust coefficients vs. TSR and wind speed and (b) difference between thrust coefficients vs. TSR and wind speed
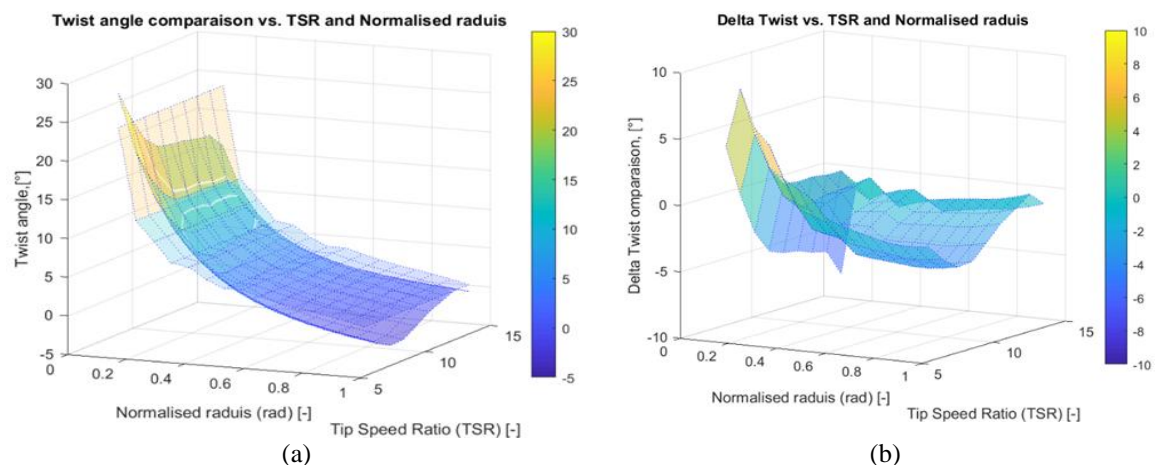

Figure 11. Local twist angle for both geometries vs. different TSR and normalized radius at a wind speed of 10 m/s (a) local twist angle vs. TSR and normalized radius and (b) difference between local twist angles vs. TSR and normalized radius

4.   CONCLUSION

The aim of this research work is to develop a smart design of HAWT. This design is based on the subdivision of the wind turbine blade to several elements. These elements are mechanically connected and enveloped by a malleable skin to ensure smooth movement. To simulate the wind turbine blade, a new algorithm based on blade element momentum method has been realized. This algorithm takes into account the local twist angle adaptation under several operating conditions. Simulation of the new design under different conditions provides significant results with high performances. The finding outcomes provide significant improvements comparing to the conventional wind turbine in terms of energy recuperation. In fact, the smart wind turbine reached maximum C_P values for a large range of TSR and wind speed. For instance, in the present study, the TSR is comprised between 6 and 14, where wind speed U_0 is comprised between 6 m/s and 14 m/s. For TSR equals 14 and U_0 equals 14 m/s, the rate of power coefficient is increased by 21%. In addition, an important attenuation of axial thrust coefficient is observed and estimated by 21%. Moreover, axial thrust coefficient is significantly decreased for high TSR values which allows preserving the mechanical structure of the wind turbine. The main achievements of the present contribution are summarized as: development of a new adaptable blade structure for the HAWT; maximization in energy recuperation over a large operating range; minimization of the axial thrust to improve the wind turbine lifetime; and optimization of the blade element root design to facilitate the wind turbine starting.

Finally, the proposed design of the wind turbine blade offers a significant investigation to improve the future wind turbines efficiency. As perspectives for the future research works, material and manufacturing techniques are suggested to develop smart wind turbine blades. To ensure smooth orientation of the blade elements, smart sensors and actuators should be used.

AUTHOR CONTRIBUTIONS STATEMENT

This journal uses the Contributor Roles Taxonomy (CRediT) to recognize individual author contributions, reduce authorship disputes, and facilitate collaboration.

Name of Author	C	M	So	Va	Fo	I	R	D	O	E	Vi	Su	P	Fu
Issam Meghlaoui	✓	✓	✓	✓	✓	✓		✓	✓		✓		✓	
Toufik Madani Layadi	✓	✓		✓	✓	✓		✓	✓	✓	✓	✓	✓	

C : **C**onceptualization	I : **I**nvestigation	Vi : **Vi**sualization
M : **M**ethodology	R : **R**esources	Su : **Su**pervision
So : **So**ftware	D : **D**ata Curation	P : **P**roject administration
Va : **Va**lidation	O : Writing - **O**riginal Draft	Fu : **Fu**nding acquisition
Fo : **Fo**rmal analysis	E : Writing - Review & **E**diting	

CONFLICT OF INTEREST STATEMENT

The authors declare that they have no known competing financial interests, personal or professional relationships that could have appeared to influence the work reported in this paper.

DATA AVAILABILITY

The data that support the findings of this study are available from the corresponding author, Toufik Madani Layadi, upon reasonable request.

REFERENCES

[1] P. J. Schubel and R. J. Crossley, "Wind turbine blade design," *Energies*, vol. 5, no. 9, pp. 3425–3449, Sep. 2012, doi: 10.3390/en5093425.

[2] T. R. Hiester and W. T. Pennell, "The meteorological aspects of siting large wind turbines," *Pacific Northwest Laboratory*, 1981.

[3] W. Z. Shen, J. N. Sørensen, and R. Mikkelsen, "Tip loss correction for actuator/navier–stokes computations," *Journal of Solar Energy Engineering*, vol. 127, no. 2, pp. 209–213, May 2005, doi: 10.1115/1.1850488.

[4] S. G. Sadler, "Method for predicting helicopter wake geometry, wake- induced flow and wake effects on blade airloads," 1972.

[5] O. Apata and D. T. O. Oyedokun, "An overview of control techniques for wind turbine systems," *Scientific African*, vol. 10, p. e00566, Nov. 2020, doi: 10.1016/j.sciaf.2020.e00566.

[6] S. Bhandari Abhi *et al.*, "An intelligent wind turbine with yaw mechanism using machine learning to reduce high-cost sensors quantity," *Indonesian Journal of Electrical Engineering and Computer Science (IJEECS)*, vol. 31, no. 1, pp. 10–21, Jul. 2023, doi: 10.11591/ijeecs.v31.i1.pp10-21.

[7] D. Kumar and K. Chatterjee, "A review of conventional and advanced MPPT algorithms for wind energy systems," *Renewable and Sustainable Energy Reviews*, vol. 55, pp. 957–970, Mar. 2016, doi: 10.1016/j.rser.2015.11.013.

[8] Q.-V. Ngo and T.-T. Nguyen, "The MPPT algorithm combined with pitch angle control for the small-scale wind turbine in a wide speed range," *International Journal of Power Electronics and Drive Systems (IJPEDS)*, vol. 12, no. 3, pp. 1482–1493, Sep. 2021, doi: 10.11591/ijpeds.v12.i3.pp1482-1493.

[9] P. Jiang, T. Zhang, J. Geng, P. Wang, and L. Fu, "An MPPT strategy for wind turbines combining feedback linearization and model predictive control," *Energies*, vol. 16, no. 10, p. 4244, May 2023, doi: 10.3390/en16104244.

[10] L. Liu, B. Zhao, and J. Hu, "Coordinated frequency control study of variable speed variable pitch of DFIG load shedding unit based on VSG," *Journal of Renewable and Sustainable Energy*, vol. 16, no. 1, Jan. 2024, doi: 10.1063/5.0168998.

[11] O. Fadi, A. Abbou, H. Mahmoudi, and S. Gaizen, "Optimized MPPT for aero-generator system built on autonomous squirrel cage generators using feed-forward neural network," *International Journal of Renewable Energy Research*, vol. 13, no. 3, pp. 1134–1144, 2023, doi: 10.20508/ijrer.v13i3.14002.g8785.

[12] E. A. Bossanyi, "Individual blade pitch control for load reduction," *Wind Energy*, vol. 6, no. 2, pp. 119–128, Apr. 2003, doi: 10.1002/we.76.

[13] L. Giammichele, V. D'Alessandro, M. Falone, and R. Ricci, "Experimental assessment of a morphing trailing edge device for wind turbine blade performance improvement," *Journal of Renewable and Sustainable Energy*, vol. 16, no. 1, Jan. 2024, doi: 10.1063/5.0174768.

[14] M. B. Farghaly and E. S. Abdelghany, "Study the effect of trailing edge flap deflection on horizontal axis wind turbine performance using computational investigation," *International Journal of Renewable Energy Research*, vol. 12, no. 4, pp. 1942–1953, 2022, doi: 10.20508/ijrer.v12i4.13433.g8617.

[15] J. Ma, Y. Chen, and M. Zhao, "Mechanism study of flow characteristics on small HAWT blade surfaces based on airfoil concavity under yaw conditions," *Journal of Renewable and Sustainable Energy*, vol. 14, no. 4, Jul. 2022, doi: 10.1063/5.0095690.

[16] A. Routray, N. Sivakumar, S. Hur, and D. Bang, "A comparative study of optimal individual pitch control methods," *Sustainability*, vol. 15, no. 14, p. 10933, Jul. 2023, doi: 10.3390/su151410933.

[17] X. Wang, J. Zhou, B. Qin, Y. Luo, C. Hu, and J. Pang, "Individual pitch control of wind turbines based on SVM load estimation and LIDAR measurement," *IEEE Access*, vol. 9, pp. 143913–143921, 2021, doi: 10.1109/ACCESS.2021.3120543.

[18] D. Song *et al.*, "A novel wind speed estimator-integrated pitch control method for wind turbines with global-power regulation," *Energy*, vol. 138, pp. 816–830, Nov. 2017, doi: 10.1016/j.energy.2017.07.033.

[19] D. C. Corbet and C. A. Morgan, "Report on the passive control of horiztonal axis wind turbines," *Control*, 1992.

[20] Y.-J. Chen and Y. Shiah, "Experiments on the performance of small horizontal axis wind turbine with passive pitch control by disk pulley," *Energies*, vol. 9, no. 5, p. 353, May 2016, doi: 10.3390/en9050353.

[21] A. Hijazi, A. ElCheikh, and M. Elkhoury, "Numerical investigation of the use of flexible blades for vertical axis wind turbines," *Energy Conversion and Management*, vol. 299, p. 117867, Jan. 2024, doi: 10.1016/j.enconman.2023.117867.

[22] G. Pechlivanoglou, "Passive and active flow control solutions for wind turbine blades," Inst. Strömungsmechanik und Technische Akustik (ISTA), 2012.

[23] M. Z. Akhter and F. K. Omar, "Review of flow-control devices for wind-turbine performance enhancement," *Energies*, vol. 14, no. 5, p. 1268, Feb. 2021, doi: 10.3390/en14051268.

[24] H. K. Nejadkhaki, A. Sohrabi, T. P. Purandare, F. Battaglia, and J. F. Hall, "A variable twist blade for horizontal axis wind turbines: Modeling and analysis," *Energy Conversion and Management*, vol. 248, p. 114771, Nov. 2021, doi: 10.1016/j.enconman.2021.114771.

[25] H. Kelele, L. Frøyd, M. Kahsay, and T. Nielsen, "Characterization of aerodynamics of small wind turbine blade for enhanced performance and low cost of energy," *Energies*, vol. 15, no. 21, p. 8111, Oct. 2022, doi: 10.3390/en15218111.

[26] M. Khaled, "Aerodynamic design and blade angle analysis of a small horizontal–axis wind turbine," *American Journal of Modern Energy*, vol. 3, no. 2, p. 23, 2017, doi: 10.11648/j.ajme.20170302.12.

[27] A. I. Altmimi, A. Aws, M. J. Jweeg, A. M. Abed, and O. I. Abdullah, "An investigation of design and simulation of horizontal axis wind turbine using QBlade," *Measurement Science Review*, vol. 22, no. 6, pp. 253–260, Dec. 2022, doi: 10.2478/msr-2022-0032.

[28] R. Özkan and M. S. Genç, "Aerodynamic design and optimization of a small-scale wind turbine blade using a novel artificial bee colony algorithm based on blade element momentum (ABC-BEM) theory," *Energy Conversion and Management*, vol. 283, p. 116937, May 2023, doi: 10.1016/j.enconman.2023.116937.

[29] S. A.R., M. C. Pandey, N. Sunil, S. N.S., V. Mugundhan, and R. K. Velamati, "Numerical study of effect of pitch angle on performance characteristics of a HAWT," *Engineering Science and Technology, an International Journal*, vol. 19, no. 1, pp. 632–641, Mar. 2016, doi: 10.1016/j.jestch.2015.09.010.

[30] H. A. Madsen, C. Bak, M. Døssing, R. Mikkelsen, and S. Øye, "Validation and modification of the blade element momentum theory based on comparisons with actuator disc simulations," *Wind Energy*, vol. 13, no. 4, pp. 373–389, May 2010, doi: 10.1002/we.359.

[31] M. Døssing, H. A. Madsen, and C. Bak, "Aerodynamic optimization of wind turbine rotors using a blade element momentum method with corrections for wake rotation and expansion," *Wind Energy*, vol. 15, no. 4, pp. 563–574, May 2012, doi: 10.1002/we.487.

[32]   W. Z. Shen, R. Mikkelsen, J. N. Sørensen, and C. Bak, "Tip loss corrections for wind turbine computations," *Wind Energy*, vol. 8, no. 4, pp. 457–475, Oct. 2005, doi: 10.1002/we.153.
[33]   M. J. Clifton-Smith, "Wind turbine blade optimisation with tip loss corrections," *Wind Engineering*, vol. 33, no. 5, pp. 477–496, Oct. 2009, doi: 10.1260/030952409790291226.
[34]   M. H. Rady, R. K. Garmode, M. Gooroochurn, and S. A. Kale, "Effect of blade root dimensions on physical and mechanical characteristics of a small wind turbine blade," *International Journal of Renewable Energy Research*, vol. 12, no. 3, pp. 1339–1346, 2022, doi: 10.20508/ijrer.v12i3.13283.g8518.
[35]   D. W. MacPhee and A. Beyene, "Performance analysis of a small wind turbine equipped with flexible blades," *Renewable Energy*, vol. 132, pp. 497–508, Mar. 2019, doi: 10.1016/j.renene.2018.08.014.
[36]   G. Gorel and M. O. Abdi, "Advanced pitch angle control based on genetic algorithm and particle swarm optimisation on FAST turbine systems," *Elektronika ir Elektrotechnika*, vol. 29, no. 4, pp. 11–18, Sep. 2023, doi: 10.5755/j02.eie.34205.
[37]   D. Wood, *Small wind turbines*. London: Springer London, 2011.
[38]   M. J. Clifton-Smith, "Aerodynamic noise reduction for small wind turbine rotors," *Wind Engineering*, vol. 34, no. 4, pp. 403–420, Jun. 2010, doi: 10.1260/0309-524X.3.4.403.

BIOGRAPHIES OF AUTHORS

Issam Meghlaoui 🆔 ⑧ SC Ⓒ was born in Annaba, Algeria. He received his engineering Diploma in electromechanical from the Department of Electromechanical Engineering, University of Annaba, Algeria in 2006. He received his Ph.D. degree in electromechanical engineering from the Department of Electromechanical of Annaba-Algeria, and ENSAM university-France in 2018. Currently, he is working as an associate Professor at the Faculty of Sciences and Technology, Department of Electromechanical, at Mohamed El Bachir El Ibrahimi University, Algeria. His research interests concern wind turbine performances, wind turbine wake, PIV investigation, and wind tunnel test. Also, he interested in HAWT modeling, fluid mechanics, wake modeling and wind turbine conversion system. He can be contacted at email: issam.meghlaoui@univ-bba.dz.

Toufik Madani Layadi 🆔 ⑧ SC Ⓒ was born in Bordj Bou Arreridj, Algeria. He received his engineering Diploma in automatic control from the Department of Electrical Engineering, University of Setif, Algeria in 2004. He obtained his Magister degree in electronics control from the Department of Electronics, University of Setif in 2007. He received his Ph.D. degree in automatic control from the Electrical Engineering Department, Setif University- Algeria, and Poitier University-France in 2016. He received his HDR diploma from the Department of Electrical Engineering, University of Setif in 2019. Currently, he is working as an associate Professor since 2009 in the Department of Electromechanical at Mohammed Elbachir El-Ibrahimi University, Bordj Bou Arreridj-Algeria. His research interests concern design and optimization of multi-source systems, and lead-acid and lithium battery technologies. Also, he interested in renewable energy sources and electric vehicles. He can be contacted at email: toufikmadani.layadi@univ-bba.dz.